Consistent description of ^{12}C and ^{16}O using a finite-range three-body interaction

N. Itagaki

Yukawa Institute for Theoretical Physics, Kyoto University, Kitashirakawa Oiwake-Cho, Kyoto 606-8502, Japan

(Received 2 September 2016; revised manuscript received 11 November 2016; published 27 December 2016)

Consistent description of ^{12}C and ^{16}O has been a long-standing problem of microscopic α cluster models, where the wave function is fully antisymmetrized and the effective interaction is applied not between α clusters but between nucleons. When the effective interaction is designed to reproduce the binding energy of ^{16}O (four α), the binding energy of ^{12}C (three α) becomes underbound by about 10 MeV. In the present study, by taking into account the coupling with the jj-coupling shell model components and utilizing the Tohsaki interaction, which is phenomenological but has finite-range three-body interaction terms, it is shown that consistent understanding of these nuclei can be achieved. The original Tohsaki interaction gives a small overbound value of about 3 MeV for ^{16}O, and this is improved by slightly modifying the three-body Majorana exchange parameter. Also, the coupling with the jj-coupling shell model wave function strongly contributes to the increase of the binding energy of ^{12}C. So far the application of the Tohsaki interaction has been limited to $4N$ nuclei; here, Bartlet and Heisenberg exchange terms are added in the two-body interaction part for the purpose of applying it to neutron-rich systems, and it is applied to ^{6}He.

DOI: 10.1103/PhysRevC.94.064324

I. INTRODUCTION

The nuclei ^{12}C and ^{16}O are typical light nuclei, and they have been extensively studied based on the cluster approaches [1]. Since there is no bound nucleus with mass number 5 or 8, formation of ^{12}C from three ^{4}He nuclei (α clusters) is a key process of the nucleosynthesis. Here, the second 0^+ state at $E_x = 7.6542$ MeV plays a crucial role, which is the second excited state of ^{12}C and is located just above the threshold energy to decay into three ^{4}He nuclei [2]. The existence of a three-α state just at this energy is an essential factor in the synthesis of various elements in stars. For ^{16}O also, cluster structure has been shown to be extremely important. Although the ground state corresponds to the doubly closed p shell of the shell model, this configuration can be also interpreted from four-α and ^{12}C $+\alpha$ viewpoints, if one takes certain limits for the intercluster distances. Also the first excited state of ^{16}O at $E_x = 6.0494$ MeV, very close to the threshold to decay into ^{12}C and ^{4}He, can be interpreted as a ^{12}C $+^{4}$He cluster state [3], and low-lying cluster states just around the threshold are quite important in the synthesis of ^{16}O in stars [4]. Various cluster models have been proposed and successfully applied to these nuclei.

However, a consistent description of ^{12}C and ^{16}O has been a long-standing problem of microscopic α cluster models. Here the definition of the microscopic model is that the wave function is fully antisymmetrized and the effective interaction is applied not between α clusters but between nucleons. When the effective interaction is designed to reproduce the binding energy of ^{16}O (four α), the binding energy of ^{12}C (three α) becomes underbound by about 10 MeV. On the other hand, when the binding energy of ^{12}C is reproduced, ^{16}O becomes overbound by about 20 MeV. The author and collaborators have previously utilized the Tohsaki interaction [5], which has finite-range three-body terms, and the obtained result is better than ones only within the two-body terms; however, the problem has not been fully solved [6].

One clue to solving this problem is the inclusion of the spin-orbit interaction. In most of the cluster models, α clusters are defined as simple a $(0s)^4$ configuration at some point. These α clusters are spin singlet systems and the spin-orbit interaction does not contribute inside α clusters and also between α clusters. In the jj-coupling shell model, the spin-orbit interaction is quite important, and this plays an essential role in explaining the observed magic numbers. According to the jj-coupling shell model, ^{12}C corresponds to the subclosure configuration of spin-orbit attractive orbits ($p_{3/2}$) and the spin-orbit interaction works attractively, whereas ^{16}O corresponds to the closure of a major shell (p shell), where both spin-orbit attractive ($p_{3/2}$) and repulsive ($p_{1/2}$) orbits are filled and the contribution of the spin-orbit interaction cancels. Therefore, inclusion of the α breaking wave function and taking into account the spin-orbit contribution are expected to decrease the binding energy difference of ^{12}C and ^{16}O. To describe the jj-coupling shell model states and include the spin-orbit contribution starting with the cluster model, the author and collaborators proposed the antisymmetrized quasicluster model (AQCM) [7–13]. In the AQCM, the transition from the cluster to shell model structure can be described by only two parameters: R representing the distance between α clusters and Λ which characterizes the transition of α cluster(s) to quasicluster(s) and quantifies the role of the spin-orbit interaction.

In nuclear structure calculations, it is quite well known that the central part of the nucleon-nucleon interaction in the calculation should have proper density dependence in order to satisfy the saturation property of nuclear systems. If one just introduces a simple two-body interaction, for instance Volkov interaction [14], which has been widely used in the cluster studies, one has to properly choose a Majorana exchange parameter for each nucleus, and consistent description of two different nuclei with the same Hamiltonian becomes tough work. Thus it is rather difficult to reproduce the threshold energies to decay into different subsystems.

Concerning the density dependence of the interaction, adding a zero-range three-body interaction term helps improve agreements with experiments, as in the modified Volkov (MV)

interaction [15]. However, in this case the binding energies become quite sensitive to the choice of the size parameter of the Gaussian-type single-particle wave function. Especially, the binding energy and radius of ^{4}He cannot be reproduced consistently. This situation is especially common in the case of the Gogny interaction widely used in mean field studies [16]. The nucleus ^{4}He is a building block of α cluster states, and it is desired that its size and binding energy be reproduced. The Tohsaki interaction, which has finite-range three-body terms, has many advantages compared with the zero-range three-body interactions. This interaction is a phenomenological one and is designed to reproduce the α-α scattering phase shift. Also it gives reasonable size and binding energy of the α cluster, which is rather difficult in the case of the zero-range three-body interaction, and the binding energy is less sensitive to the choice of the size parameter of the Gaussian-type singleparticle wave function because of the finite-range effect of the three-body interaction. Furthermore, the saturation properties of nuclear matter are reproduced rather satisfactory.

Of course, introducing a term proportional to the fractional power of the density is another possibility to reproduce the saturation properties of nuclear systems, as in density functional theories (DFTs), instead of introducing three-body interaction terms. However, in the present study, parity and angular momentum projections are performed, and also superposition of many Slater determinants is carried out based on the generator coordinate method (GCM). In this case, it is desired that the Hamiltonian be expressed in an operator form, such as a three-body interaction, which enables us to calculate the transition matrix elements between different Slater determinants. From this viewpoint, a simplified version of finite-range three-body interaction is proposed in Ref. [17].

The purpose of the present work is to combine the use of a finite-range three-body interaction for the interaction part and AQCM for the wave function part to establish consistent understanding of ^{12}C and ^{16}O. The original Tohsaki interaction gives a small overbound value for ^{16}O (about 3 MeV) [6]; here, the author tries to improve the result by slightly modifying the three-body Majorana exchange parameter. For ^{12}C, the subclosure configuration of the jj-coupling shell model, where the spin-orbit interaction plays an important role, is coupled to a three-α model space based on AQCM. For ^{16}O, the closed shell configuration of the p shell is the dominant configuration of the ground state, and the four-α model, which covers the model space of the closed p shell, is applied. Also, the application of the Tohsaki interaction has been limited to $4N$ nuclei, and Bartlet and Heisenberg exchange terms are added in the two-body interaction for the purpose of applying it to neutron-rich systems.

II. THE MODEL

A. Hamiltonian

The Hamiltonian ($\hat{H}$) consists of kinetic energy ($\hat{T}$) and potential energy ($\hat{V}$) terms,

$$\hat{H} = \hat{T} + \hat{V}, \tag{1}$$

TABLE I. Parameter set for the two-body part of the Tohsaki interaction (F1 parametrization in Ref. [5]) together with the strengths of the three-body interaction.

α	μ_α (fm)	$V_\alpha^{(2)}$ (MeV)	$V_\alpha^{(3)}$ (MeV)	$M_\alpha^{(2)}$	$W_\alpha^{(2)}$
1	2.5	-5.00	-0.31	0.75	0.25
2	1.8	-43.51	7.73	0.462	0.538
3	0.7	60.38	219.0	0.522	0.478

and the kinetic energy term is described as a one-body operator,

$$\hat{T} = \sum_i \hat{t}_i - T_{cm}, \tag{2}$$

where the center-of-mass kinetic energy (T_{cm}), which is constant, is subtracted. The potential energy has central ($\hat{V}_{\rm central}$), spin-orbit ($\hat{V}_{\rm spin\text{-}orbit}$), the Coulomb parts.

B. Tohsaki Interaction

For the central part of the potential energy ($\hat{V}_{\rm central}$), the Tohsaki interaction is adopted. The Tohsaki interaction consists of two-body ($V^{(2)}$) and three-body ($V^{(3)}$) terms:

$$\hat{V}_{\rm central} = \frac{1}{2}\sum_{i\neq j} V_{ij}^{(2)} + \frac{1}{6}\sum_{i\neq j, j\neq k, i\neq k} V_{ijk}^{(3)}, \tag{3}$$

where $V_{ij}^{(2)}$ and $V_{ijk}^{(3)}$ consist of three terms,

$$V_{ij}^{(2)} = \sum_{\alpha=1}^{3} V_\alpha^{(2)} \exp\left[-(\vec{r}_i - \vec{r}_j)^2/\mu_\alpha^2\right]\left(W_\alpha^{(2)} + M_\alpha^{(2)} P^r\right)_{ij}, \tag{4}$$

$$V_{ijk}^{(3)} = \sum_{\alpha=1}^{3} V_\alpha^{(3)} \exp\left[-(\vec{r}_i - \vec{r}_j)^2/\mu_\alpha^2 - (\vec{r}_i - \vec{r}_k)^2/\mu_\alpha^2\right] \times \left(W_\alpha^{(3)} + M_\alpha^{(3)} P^r\right)_{ij}\left(W_\alpha^{(3)} + M_\alpha^{(3)} P^r\right)_{ik}. \tag{5}$$

Here, P^r represents the exchange of the spatial part of the wave functions of interacting two nucleons, and this is equal to $-P^\sigma P^\tau$ due to the Pauli principle ($P^r P^\sigma P^\tau = -1$), where P^σ and P^τ are spin and isospin exchange operators, respectively. The range parameters $\{\mu_\alpha\}$ are set to be common for the two-body and three-body parts, and the values are listed in Table I together with strengths of two-body interaction $\{V_\alpha^{(2)}\}$, three-body interaction $\{V_\alpha^{(3)}\}$, and the Majorana exchange parameters of the two-body interaction. The values of Winger parameters, $\{W_\alpha^{(2)}\}$, are given as $W_\alpha^{(2)} = 1 - M_\alpha^{(2)}$. The F1 parameter set in Ref. [5] is employed. The Majorana exchange parameters for three-body interaction terms are shown in Table II.

Until now, the Tohsaki interaction has been applied only to $4N$ nuclei, and in this article the application to neutron-rich nuclei is shown. The original Tohsaki interaction does have Wigner and Majorana exchange terms, but spin and isospin exchange terms are missing. Because of this, the interaction gives a weak bound state for a two-neutron system, as in the case of Volkov interaction. Therefore, here Bartlet (BP^σ) and Heisenberg (HP^τ) exchange terms are added in Eq. (4) as

TABLE II. Majorana exchange parameters for the three-body interaction terms. F1 stands for the original F1 set of the Tohsaki interaction [5], and F1′ is the modified versions introduced in the present article.

	F1	F1′
$M_1^{(3)}$	0.0	0.0
$M_2^{(3)}$	0.0	0.0
$M_3^{(3)}$	1.909	1.5

$(W_\alpha^{(2)} + BP^\sigma - HP^\tau + M_\alpha^{(2)}P^r)_{ij}$. The values of B and H are chosen to be 0.1. By adding these terms, the neutron-neutron interaction (or proton-proton interaction) becomes weaker than the original interaction, while the α-α scattering phase shift is not influenced by this modification.

C. Spin-orbit interaction

For the spin-orbit part, G3RS [18], which is a realistic interaction originally determined to reproduce the nucleon-nucleon scattering phase shift, is adopted:

$$\hat{V}_{\text{spin-orbit}} = \frac{1}{2}\sum_{ij} V_{ij}^{ls}, \tag{6}$$

$$V_{i\neq j}^{ls} = V_{ls}(e^{-d_1(\vec{r}_i-\vec{r}_j)^2} - e^{-d_2(\vec{r}_i-\vec{r}_j)^2})P(^3O)\vec{L}\cdot\vec{S}, \tag{7}$$

where $d_1 = 5.0$ fm^{-2}, $d_2 = 2.778$ fm^{-2}, and $P(^3O)$ is a projection operator onto a triplet odd state. The operator $\vec{L}$ stands for the relative angular momentum and $\vec{S}$ is the total spin, ($\vec{S} = \vec{S}_1 + \vec{S}_2$). The strength, V_{ls}, has been determined to reproduce the ^{4}He$+n$ scattering phase shift [19], and $V_{ls} =$ 1600–2000 MeV has been suggested.

D. Single-particle wave function (Brink model)

In conventional α cluster models, the single-particle wave function has a Gaussian shape [20]:

$$\phi_i = \left(\frac{2\nu}{\pi}\right)^{\frac{3}{4}} \exp[-\nu(\boldsymbol{r}_i - \boldsymbol{R}_i)^2]\eta_i, \tag{8}$$

where η_i represents the spin-isospin part of the wave function, and $\boldsymbol{R}_i$ is a real parameter representing the center of a Gaussian wave function for the ith particle. In the Brink-Bloch wave function, four nucleons in one α cluster share a common $\boldsymbol{R}_i$ value. Hence, the contribution of the spin-orbit interaction vanishes.

E. Single-particle wave function in the AQCM

In the AQCM, α clusters are changed into quasiclusters. For nucleons in the quasicluster, the single-particle wave function is described by a Gaussian wave packet, and the center of this packet $\boldsymbol{\zeta}_i$ is a complex parameter:

$$\psi_i = \left(\frac{2\nu}{\pi}\right)^{\frac{3}{4}} \exp[-\nu(\boldsymbol{r}_i - \boldsymbol{\zeta}_i)^2]\chi_i\tau_i, \tag{9}$$

where χ_i and τ_i in Eq. (9) represent the spin and isospin parts of the ith single-particle wave function, respectively. The spin orientation is governed by the parameters $\xi_{i\uparrow}$ and $\xi_{i\downarrow}$, which are in general complex, while the isospin part is fixed to be "up" (proton) or "down" (neutron):

$$\chi_i = \xi_{i\uparrow}|\uparrow\rangle + \xi_{i\downarrow}|\downarrow\rangle, \qquad \tau_i = |p\rangle \text{ or } |n\rangle. \tag{10}$$

The center of the Gaussian wave packet is given as

$$\boldsymbol{\zeta}_i = \boldsymbol{R}_i + i\Lambda \boldsymbol{e}_i^{\text{spin}} \times \boldsymbol{R}_i, \tag{11}$$

where $\boldsymbol{e}_i^{\text{spin}}$ is a unit vector for the intrinsic-spin orientation, and Λ is a real control parameter describing the dissolution of the α cluster. As one can see immediately, the $\Lambda = 0$ AQCM wave function, which has no imaginary part, is the same as the conventional Brink-Bloch wave function. The AQCM wave function corresponds to a jj-coupling shell model wave function, such as the subshell closure configuration, when $\Lambda = 1$ and $\boldsymbol{R}_i \to 0$. The mathematical explanation for this is summarized in Ref. [11]. For the width parameter, the value of $\nu = 0.23$ fm^{-2} is used.

F. AQCM wave function of the total system

The wave function of the total system Ψ is the antisymmetrized product of these single-particle wave functions:

$$\Psi = \mathcal{A}\{\psi_1\psi_2\psi_3\cdots\cdot\psi_A\}. \tag{12}$$

The projections onto parity and angular momentum eigenstates can be performed by introducing the projection operators P_{MK}^J and P^π, and these are performed numerically in the actual calculation.

G. Superposition of different configurations

Based on GCM, the superposition of different AQCM wave functions can be done:

$$\Phi = \sum_i c_i P_{MK}^J P^\pi \Psi_i. \tag{13}$$

Here, $\{\Psi_i\}$ is a set of AQCM wave functions with different values of the R and Λ parameters, and the coefficients for the linear combination, $\{c_i\}$, are obtained by solving the Hill-Wheeler equation [20]. A set of coefficients for the linear combination $\{c_j\}$ for each eigenvalue of E is determined in this way.

III. RESULTS

Before showing the applications, here let us discuss the size parameter [ν in Eq. (9)] dependence on the ^{4}He energy, with the $(0s)^4$ configuration calculated using the Tohsaki interaction. As mentioned in the Introduction, the size parameter dependence is quite small because of the finite-size effect of the three-body interaction, compared with the zero-range three-body interaction cases. Here the F1 parameter set of the Tohsaki interaction is adopted. In Fig. 1, the energy minimum point appears at $\nu = 0.25$ fm^{-2} and the curvature is rather flat around this point. Later the F1′ parameter set will be newly introduced, but the result for ^{4}He with the $(0s)^4$ configuration does not change.

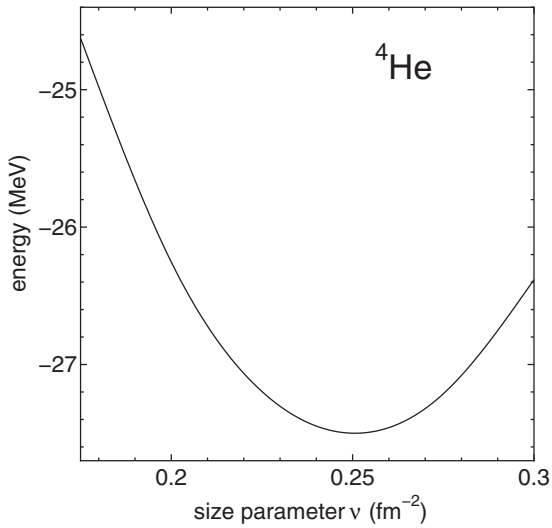

FIG. 1. The size parameter [ν in Eq. (9)] dependence on the ^{4}He energy with the $(0s)^4$ configuration calculated using the Tohsaki interaction. The F1 parameter set is adopted.

The application of Tohsaki interaction starts with ^{6}He. So far the Tohsaki interaction has been applied to $4N$ nuclei, but here a neutron-rich system is examined. Figure 2 shows the energy convergence of the ground 0^+ state of ^{6}He [ν in Eq. (9) is set to 0.23 fm^{-2}]. The model space is $\alpha + n + n$ and the positions of the two neutrons are randomly generated, and different configurations for the neutrons are superposed. The dot-dashed line at -27.31 MeV shows the threshold energy of ^{4}He $+n + n$ (the experimental value is $-28.295\,66$ MeV).

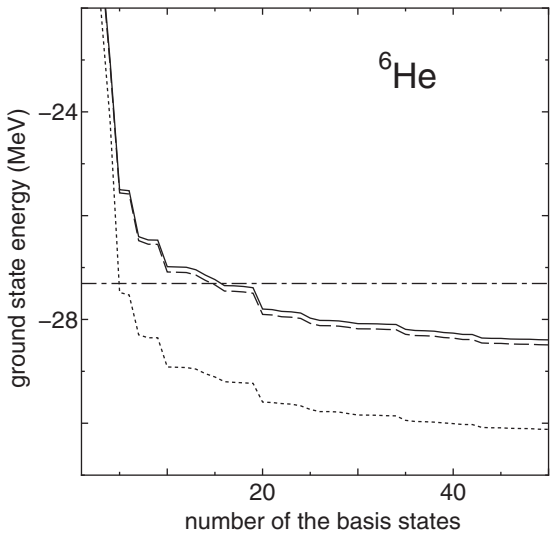

FIG. 2. The energy convergence of the ground 0^+ state of ^{6}He with an $\alpha + n + n$ model. Different configurations for the two neutrons outside ^{4}He are superposed. The horizontal line at -27.31 MeV shows the threshold energy of ^{4}He $+n + n$. The dotted line is the result of original F1 parameter set, and the dashed line is the result after adding $B = H = 0.1$. The result of the F1′ parameter set is shown as the solid line.

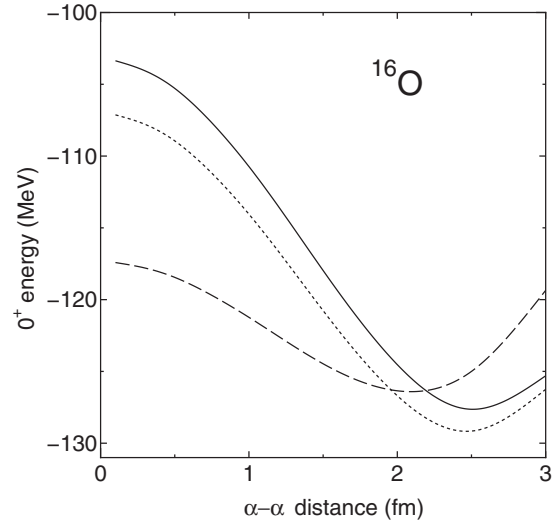

FIG. 3. The 0^+ energy of ^{16}O with a tetrahedron configuration of four α's as a function of distance between α clusters. The dotted line is the result of the original F1 parameter set. The result of the F1′ parameter set is shown as the solid line. The dashed line is for the result calculated using the Volkov No. 2 interaction [14] with $M = 0.63$.

Here, the dotted line is the result of original F1 parameter set. The Bartlet and Heisenberg terms are added with the parameters of $B = H = 0.1$, and the result is shown as the dashed line. Furthermore, the Majorana exchange parameter of the three-body interaction term is slightly modified and the result of the F1′ parameter set (defined in Table II) is shown as solid line (this is to reproduce the binding energy of ^{16}O, which will be discussed shortly). For the spin-orbit part, the strength V_{ls} has been determined to be 1600–2000 MeV in the analysis of the ^{4}He $+n$ scattering phase shift [19], and here $V_{ls} = 1600$ MeV is adopted. The results of dashed and solid lines are similar and difficult to distinguish. Nevertheless, by adding Bartlet and Heisenberg terms, a binding energy close to the experimental one is obtained (the experimental value of S_{2n} is 0.975 MeV).

For ^{16}O, according to the jj-coupling shell model, the ground state corresponds to the closure of a major shell (p shell), where both spin-orbit attractive ($p_{3/2}$) and repulsive ($p_{1/2}$) orbits are filled and the contribution of the spin-orbit interaction cancels. Therefore, α breaking configurations are not expected to mix strongly, and here a four-α model space is introduced, which is known to coincide with the closed p shell configuration at the limit of relative distance between α clusters equal to zero. The 0^+ energy of ^{16}O with a tetrahedron configuration of four α's is shown in Fig. 3 as a function of the relative distance between α clusters [ν in Eq. (9) is set to 0.23 fm^{-2}]. The dotted line is the result of the original F1 parameter set, and the result of the newly introduced F1′ parameter set (defined in Table II) is shown as the solid line. Here, F1′ is designed to avoid the small overbinding of ^{16}O when the original F1 parameter set is introduced, and the solid line is less attractive compared with the dotted line by about 2–3 MeV. The eigenenergy of ^{16}O is obtained by superposing

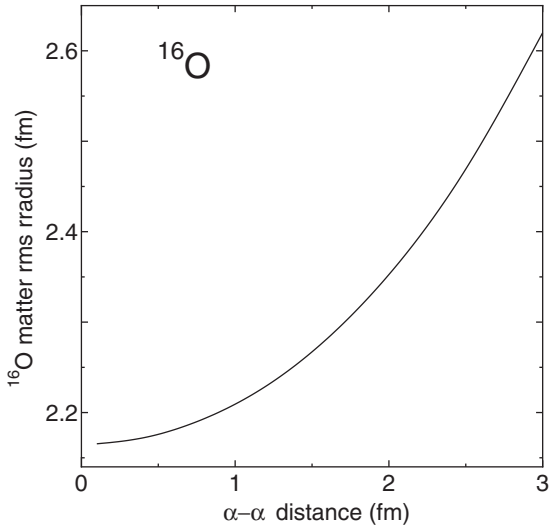

FIG. 4. The matter point rms radius for the 0^+ state of ^{16}O calculated with the tetrahedron configuration of four α's. The horizontal axis shows the relative distance between α clusters.

the basis states with α-α distances of 0.1, 0.5, 1.0, 1.5, 2.0, 2.5, and 3.0 fm based on GCM, and the newly introduced F1′ parameter set gives -127.9 MeV for the ground state compared to the experimental value of $-127.619\,293$ MeV.

The observed root mean square (rms) radius of ^{16}O is quite large: the charge radius is 2.69 fm [21], and the radius is often underestimated by 0.1–0.2 fm, if one calculates with four-α models and uses only a two-body effective interaction such as the Volkov interaction [14]. The dashed line in Fig. 3 is for the result calculated using the Volkov No. 2 interaction with $M = 0.63$. In this case, the energy curve is much shallower, and features of the curve are quite different from the Tohsaki interaction cases. The dashed line shows the energy minimum point around an α-α distance of 2 fm. Using the Tohsaki interaction with finite-range three-body interaction terms, the solid line in Fig. 3 shows that the lowest energy is obtained with an α-α distance of 2.5 fm, larger than the result of the Volkov interaction (dashed line) by 0.5 fm. The matter point rms radius for the 0^+ state of ^{16}O with a tetrahedron configuration of four α's is shown in Fig. 4 as a function of distance between α clusters. When the α-α distance is 2.5 fm, which gives the lowest energy in the Tohsaki interaction cases, the matter point radius is 2.49 fm. This matter point radius decreases to 2.35 fm if the α-α distance is 2.0 fm, which gives the lowest energy in the Volkov interaction case. The ground state of ^{16}O obtained by superposing the basis states with the α-α distances of 0.1, 0.5, 1.0, 1.5, 2.0, 2.5, and 3.0 fm gives a matter pont rms matter radius of 2.49 fm (Tohsaki interaction F1′ parameter set). This value corresponds to a charge radius of 2.64 fm, and the experimental value is almost reproduced.

It is important to show not only the energy curvature with respect to α-α distance but also the size parameter dependence on the energy and charge radius of ^{16}O. The ^{16}O wave functions with tetrahedron configuration of four α's are superposed and the energy and charge radius of the ground state are obtained, where the size parameter ν [defined in Eq. (9)] of the Gaussian-type single-particle orbit is changed. In Table III, Energy and Radius stand for the energy and charge radius (fm) of the ground state. The size parameter dependence is rather small, and this is again coming from the finite-size effect of the three-body interaction in the present model.

TABLE III. Size parameter dependence on the energy and charge radius of ^{16}O. Energy and Radius stand for the energy and charge radius of the ground state as a function of the size parameter ν [defined in Eq. (9)] of the Gaussian-type single-particle orbit. Expt. denotes experimental values.

ν (fm^{-2})	0.17	0.20	0.23	0.26	Expt.
Energy (MeV)	-124.1	-128.0	-127.9	-124.2	-127.6
Radius (fm)	2.79	2.70	2.64	2.57	2.69

Here the F1 (original) and F1′ (modified) parameter sets of the Tohsaki interaction are compared. The 0^+ energy curves of α-α (^{8}Be) calculated with F1 (dotted line) and F1′ (solid line) are compared in Fig. 5. As explained previously, F1′ is designed to avoid small overbinding of ^{16}O calculated with F1, and the solid line is slightly more repulsive at short α-α relative distances. However, the difference is quite small, less than 1 MeV, and the character of the original F1 that reproduces the α-α scattering phase shift is not influenced by this modification.

For ^{12}C, jj-coupling (α breaking) components of the wave function are needed, and these are prepared based on AQCM. Basis states with equilateral triangular configuration of three α clusters with relative distances of $R = 0.5$, 1.0, 1.5, 2.0, 2.5, and 3.0 fm are introduced, and α clusters are changed to quasiclusters by giving the dissolution parameter Λ. The values of Λ are chosen to be 0.2 and 0.4, since the states in between pure three-α clusters ($\Lambda = 0$) and

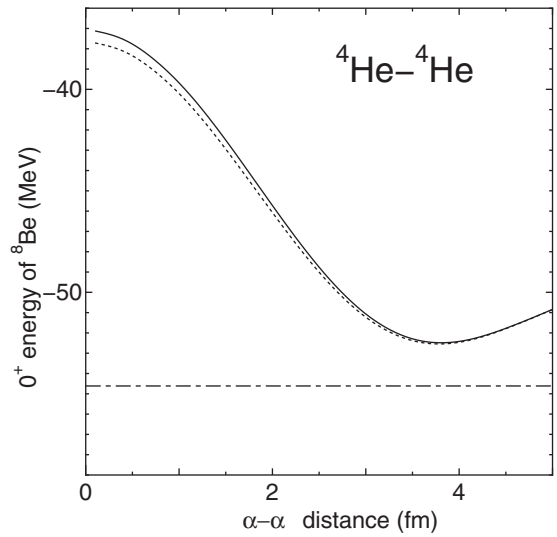

FIG. 5. The 0^+ energy curves of ^{8}Be calculated with the $\alpha + \alpha$ model as a function of relative α-α distance. The dotted and solid lines are the results calculated with the original F1 parameter set and newly introduced F1′ parameter set. The dot-dashed line at -54.61 MeV shows the threshold energy of $\alpha + \alpha$.

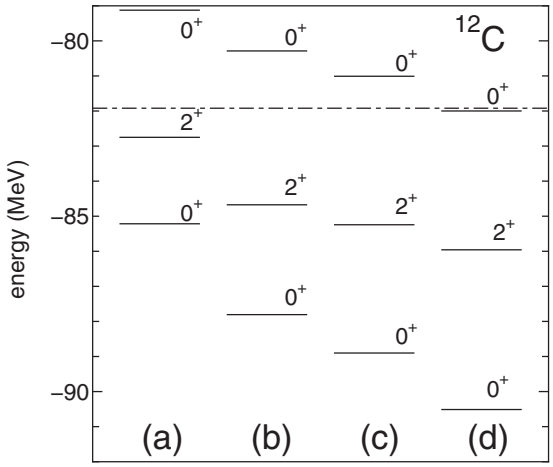

FIG. 6. The energy levels of ^{12}C. Here (a) is the result without the spin-orbit interaction, and (b), (c), and (d) show the results calculated with 1600, 1800, and 2000 MeV for the strength of the spin-orbit terms of the G3RS interaction [V_{ls} in Eq. (7)], respectively. The dot-dashed line at −81.92 MeV shows the three-α threshold energy.

the jj-coupling shell model limit ($\Lambda = 1$) are known to be important for the description of the ground state. In addition to these 12 basis states, 28 more basis states with various three-α configurations are introduced by randomly generating Gaussian center parameters. This is because the Hoyle state is a gaslike state without specific shape, and it has been known that not only equilateral triangular configuration but various three-α cluster configurations couple in this state. The ν value in Eq. (9) is set to 0.23 fm^{-2}.

By superposing these 40 basis states based on GCM and diagonalizing the Hamiltonian, energy eigenstates are obtained. The F1′ parameter set of the Tohsaki interaction is adopted for the central part. In Fig. 6, the ground 0$^+$, first 2$^+$, and second 0$^+$ states of ^{12}C are shown together with the calculated three-α threshold energy (dot-dashed line). The strength of the spin-orbit interaction, V_{ls} in Eq. (7), is chosen as $V_{ls} = 0$, 1600, 1800, and 2000 MeV in (a), (b), (c), and (d), respectively. The reasonable range of the strength of $V_{ls} = 1600$–2000 MeV has been suggested in the ^{4}He $+n$ scattering phase shift analysis [19]. Without the spin-orbit interaction ($V_{ls} = 0$ MeV), the ground 0$^+$ state of ^{12}C is obtained at −85.2 MeV in Fig. 6(a), compared with the experimental value of −92.161 726 MeV. However, with the spin-orbit effect, the ground state is obtained at −87.8 MeV in Fig. 6(b) ($V_{ls} = 1600$ MeV), −88.9 MeV in (c) ($V_{ls} = 1800$ MeV), and −90.5 MeV in (d) ($V_{ls} = 2000$ MeV). Therefore, the absolute value of the binding energy of ^{12}C can be almost reproduced with the present interaction and the model, together with the binding energies of ^{4}He and ^{16}O. If one measures the energy from the three-α threshold energy, the ground state of ^{12}C is −3.3 MeV in Fig. 6(a), −5.9 MeV in (b), −7.0 MeV in (c), and −8.6 MeV in (d), compared with the experimental value of −7.2747 MeV. Thus the binding energy from the three-α threshold is also reproduced in the case of $V_{ls} = 1800$ MeV [Fig. 6(c)].

TABLE IV. The calculated $B(E2)$ values of ^{12}C (e^2fm^4) from the first 2$^+$ state to the ground state [$B(E2\ 2^+_1 \to 0^+_1)$] and that from the second 0$^+$ state to the first 2$^+$ state [$B(E2\ 0^+_2 \to 2^+_1)$] as a function of strength of the spin-orbit interaction, V_{ls} (MeV), in Eq. (7). Expt. stands for the experimental values [25].

V_{ls}	0	1600	1800	2000	Expt.
$B(E2\ 2^+_1 \to 0^+_1)$	18.3	10.7	8.67	6.54	7.8 ± 0.4
$B(E2\ 0^+_2 \to 2^+_1)$	9.27	14.5	18.3	21.8	13 ± 4

The famous Hoyle state, the second 0$^+$ state experimentally observed at $E_x = 7.65420$ MeV, appears at $E_x = 6.1$ MeV in Fig. 6(a), $E_x = 7.5$ MeV in (b), $E_x = 7.9$ MeV in (c), and $E_x = 8.6$ MeV in (d). If one measures from the three-α threshold energy, these energies correspond to $E_x = 2.8$ MeV in Fig. 6(a), $E_x = 1.6$ MeV in (c), $E_x = 0.9$ MeV in (c), and $E_x = -0.1$ MeV in (d). Here again $V_{ls} = 1800$ MeV gives reasonable agreements with the experiment. However the result implies that a slightly larger number of basis states are needed to reproduce Hoyle state just above (experimentally 0.38 MeV) the three-α threshold energy.

The calculated point matter radii of the first and second 0$^+$ states of ^{12}C are 2.42 fm (corresponding to the charge radius of 2.56 fm compared with the experimental value of 2.47 fm) and 3.05 fm, respectively. The values for the fermionic molecular dynamics (FMD) calculation [22] are 2.39 and 3.38 fm, respectively. The second 0$^+$, which is much extended compared with the ground state, is successfully obtained in the present model; however, more basis states would be needed for a quantitative description of the gaslike nature.

The traditional three-α cluster models have a serious problem: they give very small level spacing between the ground 0$^+$ state and the first 2$^+$ state, which is the first excited state of ^{12}C [1]. In the present case, the $V_{ls} = 0$ MeV result in Fig. 6(a) shows that the level spacing is 2.5 MeV, which is much smaller than the experimental value of 4.438 913 1 MeV. This is improved by the spin-orbit effect, since the excitation from the ground 0$^+$ state to the 2$^+$ state corresponds to one-particle–one-hole excitation to a spin-orbit unfavored orbit from the closure configuration of spin-orbit attractive orbits in the jj-coupling shell model. The 0$^+$–2$^+$ level spacing becomes 3.1 MeV in (b), 3.7 MeV in (c), and 4.6 MeV in (c). A similar trend has been reported in the recent antisymmetrized molecular dynamics (AMD) [23] and FMD [22,24] calculations.

The calculated $B(E2)$ values of ^{12}C (e^2fm^4) from the first 2$^+$ state to the ground state [$B(E2\ 2^+_1 \to 0^+_1)$] and that from the second 0$^+$ state to the first 2$^+$ state [$B(E2\ 0^+_2 \to 2^+_1)$] are listed in Table IV as a function of strength of the spin-orbit interaction, V_{ls}, in Eq. (7). With increasing strength of the spin-orbit interaction, mixing of the α breaking components becomes important, and the $B(E2\ 2^+_1 \to 0^+_1)$ value decreases, whereas the $B(E2\ 0^+_2 \to 2^+_1)$ value increases, as indicated in our previous work [26] and in AMD [23] and FMD [12,24] calculations. Comparing with the experimental values, again $V_{ls} \sim 1800$ MeV is confirmed to be a reasonable choice.

The appearance of negative parity states in low-lying excitation energy has been considered the signature of the importance of the three-α cluster structure in ^{12}C. Experimentally, 3^- and 1^- states have been observed at $E_x = 9.6415$ MeV and $E_x = 10.84416$ MeV, respectively. These 3^- and 1^- states are reproduced at 9.8 and 12.6 MeV, respectively, when the strength of the spin-orbit interaction is chosen as $V_{ls} = 1800$ MeV, which gives reasonable results for the 0^+ and 2^+ states.

IV. SUMMARY

The consistent description of ^{12}C and ^{16}O, which has been a long-standing problem of the microscopic cluster model, is examined. By taking into account the coupling with the jj-coupling shell model and utilizing the Tohsaki interaction, which is a finite-range three-body interaction, consistent understanding of these nuclei can be achieved. The original Tohsaki interaction gives a small overbound value of about 3 MeV for ^{16}O, and this is improved by slightly modifying the three-body Majorana exchange parameter. Also, so far the application of the Tohsaki interaction has been limited to $4N$ nuclei; here, Bartlet and Heisenberg exchange terms are added in the two-body interaction for the purpose of applying it to neutron-rich systems.

By applying the Tohsaki interaction with finite-range three-body interaction terms to ^{16}O, the lowest energy of the tetrahedron configuration of four α's is obtained with very large α-α distance (2.5 fm). After performing GCM, the ground state is obtained with a charge radius of 2.64 fm, compared with the observed value of 2.69 fm. The radius is often underestimated by 0.1–0.2 fm with four-α models, if one calculates only within the two-body effective interactions, and this is significantly improved.

For ^{12}C, various α configurations are prepared by randomly generating Gaussian center parameters, and jj-coupling (α breaking) components are mixed based on AQCM. The ground 0^+ state of ^{12}C is obtained in the range -88.0 to -90.5 MeV with reasonable strength of the spin-orbit interaction, compared with the experimental value of -92.2 MeV. The absolute value of the binding energy of ^{12}C (and also ^{4}He and ^{16}O) can be almost reproduced with the present interaction and the model. If one measures the energy from the three-α threshold energy, the agreement with the experiment is even more reasonable. The famous Hoyle state (second 0^+ state) is reproduced just around the three-α threshold energy. Also, traditional three-α cluster models give very small level spacings for the ground 0^+ state and the first 2^+ state, and this is significantly improved by the spin-orbit effect. The $B(E2)$ values from the first 2^+ state to the ground state and that from the second 0^+ state to the first 2^+ state also show the importance of the spin-orbit effect. The appearance of negative parity states at low-lying excitation energy has been considered the signature of the three-α cluster structure of ^{12}C. Experimentally 3^- and 1^- states have been observed at $E_x = 9.6415$ MeV and $E_x = 10.84416$ MeV, respectively, and these states are also reproduced within the present framework (9.8 and 12.6 MeV, respectively).

ACKNOWLEDGMENTS

The author thanks the discussions with Prof. A. Tohsaki. Numerical calculation has been performed at Yukawa Institute for Theoretical Physics, Kyoto University. This work was supported by JSPS KAKENHI Grant No. 716143900002.

[1] Y. Fujiwara *et al.*, Prog. Theor. Phys. Suppl. **68**, 29 (1980).
[2] F. Hoyle, Astrophys. J. Suppl. Ser. **1**, 121 (1954).
[3] H. Horiuchi and K. Ikeda, Prog. Theor. Phys. **40**, 277 (1968).
[4] P. Descouvemont, Phys. Rev. C **47**, 210 (1993).
[5] A. Tohsaki, Phys. Rev. C **49**, 1814 (1994).
[6] N. Itagaki, A. Ohnishi, and K. Katō, Prog. Theor. Phys. **94**, 1019 (1995).
[7] N. Itagaki, H. Masui, M. Ito, and S. Aoyama, Phys. Rev. C **71**, 064307 (2005).
[8] H. Masui and N. Itagaki, Phys. Rev. C **75**, 054309 (2007).
[9] T. Yoshida, N. Itagaki, and T. Otsuka, Phys. Rev. C **79**, 034308 (2009).
[10] N. Itagaki, J. Cseh, and M. Płoszajczak, Phys. Rev. C **83**, 014302 (2011).
[11] T. Suhara, N. Itagaki, J. Cseh, and M. Płoszajczak, Phys. Rev. C **87**, 054334 (2013).
[12] T. Suhara and Y. Kanada-En'yo, Phys. Rev. C **91**, 024315 (2015).
[13] N. Itagaki, H. Matsuno, and T. Suhara, Prog. Theor. Exp. Phys. **2016**, 093D01 (2016).
[14] A. B. Volkov, Nucl. Phys. **74**, 33 (1965).
[15] T. Ando, K. Ikeda, and A. Tohsaki-Suzuki, Prog. Theor. Phys. **64**, 1608 (1980).
[16] J. Decharge and D. Gogny, Phys. Rev. C **21**, 1568 (1980).
[17] Y. Kanada-En'yo and Y. Akaishi, Phys. Rev. C **69**, 034306 (2004).
[18] R. Tamagaki, Prog. Theor. Phys. **39**, 91 (1968).
[19] S. Okabe and Y. Abe, Prog. Theor. Phys. **61**, 1049 (1979).
[20] D. M. Brink, in *Proceedings of the International School of Physics "Enrico Fermi" Course XXXVI*, edited by C. Bloch (Academic, New York, 1966), p. 247.
[21] I. Angeli and K. P. Marinova, At. Data Nucl. Data Tables **99**, 69 (2013).
[22] M. Chernykh, H. Feldmeier, T. Neff, P. von Neumann-Cosel, and A. Richter, Phys. Rev. Lett. **98**, 032501 (2007); **105**, 022501 (2010).
[23] Y. Kanada-En'yo, Phys. Rev. Lett. **81**, 5291 (1998); Prog. Theor. Phys. **117**, 655 (2007).
[24] T. Neff and H. Feldmeier, Nucl. Phys. A **738**, 357 (2004).
[25] F. Ajzenberg-Selove, Nucl. Phys. A **248**, 1 (1975).
[26] N. Itagaki, K. Hagino, T. Otsuka, S. Okabe, and K. Ikeda, Nucl. Phys. A **719**, C205 (2003).